

Received March 19, 2020, accepted April 20, 2020, date of publication April 23, 2020, date of current version May 8, 2020.

Digital Object Identifier 10.1109/ACCESS.2020.2989831

Information Entropy Multi-Decision Attribute Reduction Fuzzy Rough Set for Dust Particulate Imagery Characteristic Extraction

ZHENG WANG¹, XU ZHENG², HONGGUANG PAN¹, AND DONGYAN LI¹

¹College of Electrical and Control Engineering, Xi'an University of Science and Technology, Xi'an 710054, China

²Shaanxi Institute for Food and Drug Control, Xi'an 710065, China

Corresponding author: Hongguang Pan (hongguangpan@163.com)

This work was supported in part by the National Natural Science Foundation of China under Grant 51804249, in part by the Outstanding Youth Science Fund of Xi'an University of Science and Technology under Grant 2018YQ2-07, in part by the Shaanxi Postdoctoral Science Foundation under Grant 2018BSHEDZZ124, and in part by the China Postdoctoral Science Foundation under Grant 2017M623207.

ABSTRACT High-precision extraction of particulate characteristic modes is essential for dust explosion safety measurements, such as particulate concentration and size distribution. A new solution based on information entropy multi-decision attribute reduction fuzzy rough set is proposed to analyse the particulate morphology characteristics, which effectively avoids the shortcomings of traditional technology (low accuracy, stochasticity, etc.). The proposed approach consists of three stages: membership function modelling, attribute reduction, and maximum information entropy threshold segmentation. The membership coefficient was determined with a multi-segment function by developing the fuzzy degree of the membership model for dust image pixels. The fuzzy dependence of the conditional attribute was determined to extract the fuzzy attribute reduction. Finally, the model of coal dust particulates with information entropy was improved to extract the maximum segmentation threshold, which is significant for classification. The proposed methods were evaluated over a sequence of 30 image sets. The unclassified rate evaluation reached 0.978 for particle sizes $\geq 200 \mu\text{m}$, 0.958 for $[75 \mu\text{m}, 200 \mu\text{m}]$ and 0.950 for particle sizes $< 75 \mu\text{m}$. The proposed reduction approach offered a performance improvement in terms of more important attribute implementation. The paper demonstrated that the maximum information entropy reduction model can remove the redundant attributes without compromising the precision.

INDEX TERMS Fuzzy membership, image grey feature, information entropy, multi-attribute reduction.

I. INTRODUCTION

With increasing attention being paid by state and relevant experts to environmental pollution caused by substantial coal mining, coal dust recognition technology based on imagery information is attracting more extensive and in-depth studies in mines locally and abroad because of its efficient visualization and intelligent application [1], [2]. Technology to extract the visual information from imagery can solve safety issues in coal mines, provide an effective and highly reliable way to adapt to adverse environments, and accurately predict coal dust explosion hazards. However, the dust detection mechanism is extremely complex, and there are many determinants, resulting in significant randomness of the coal dust detection

results. With the decrease in dust particulate dispersivity, it becomes increasingly common to find a cell at a certain resolution that contains only a few local details. The statistics indicate that data with low and median resolution are no longer applicable to model the global properties of high-resolution dust images. Therefore, the major work of this paper focuses on how to extract discriminative features for image classification [3].

Therefore, many studies conducted locally have focused on the development of dust particulate detection mechanisms, resulting in many varied findings. Recently, a light scattering approach was introduced by Okpeafoh *et al.* [4] to address the difficulty of obtaining instantaneous dust concentration changes, but only ideal spherical particulates could be taken as the test standard. The method that could detect non-spherical coal dust particulates exhibited deviations and

The associate editor coordinating the review of this manuscript and approving it for publication was Jenny Mahoney.

caused particulate shape measurement errors. Sun *et al.* [5] thought that β -rays are not affected by factors such as dust type, particle size, dispersion, shape, and colour. Consequently, they utilized the advantages of the β -ray measurement method to achieve automatic continuous detection of dust concentrations with high measurement accuracy. However, this method was inefficient and exhibited potential safety problems with strong radiation sources [6].

Considering the limitations of technical methods and research perspectives, the abovementioned studies did not systematically analyse the characteristics of coal dust particulates. With the development of research methods, coal dust recognition technology based on imagery information has the advantage of being able to directly observe various coal dust particle sizes and shapes. Alpana [7] proposed dividing the coal dust imagery regions with different characteristics according to grey similarity and discontinuity. The characteristic parameters of particulate targets were measured, and the particulate features were extracted. The obtained research results have important reference value that can be used for further studies. Omid *et al.* [8] applied a maximum entropy automatic threshold to deal with various image signal-to-noise ratios in the imagery space. This method could produce satisfactory extraction effects because of its high sensitivity to the image contrast and histogram distribution performance. However, this method ignored the spatial information between image targets with little grey value differences and the conditions of overlapping grey value areas. The histograms did not have obvious double peaks; thus, the extraction effect was poor [9]. The above research method considered the distribution of imagery greyscale space more effectively than other methods, greatly improving the accuracy of image extraction. However, this method cannot achieve an ideal situation indefinitely. An issue that needs to be discussed is how to use reasonable research means to effectively explain the microscopic characteristics of the appearance of coal dust particulates based on spatial information in images [10], [11].

Through the research on imagery space theory and micro-science, it was found that the information characteristics of coal dust particulates can be addressed using nonlinear and uncertainty modelling [12]. Furthermore, the difficulty in image recognition lies in the accuracy of redundant feature removal. In this study, the image characteristics of coal dust particulates were researched from a microscopic perspective. Multi-attribute reduction provides a new solution to this problem [13]. The proposed approach consists of two major parts: multi-segment membership determination and information entropy attribute reduction [14], [15]. In the first part, based on the division of regional spatial information based on the image greyscale characteristics, the classification and selection of attribute importance is presented. Local details are modelled, and several multi-segment functions are utilized to extract local features of images. The most important steps are determining an appropriate number of membership coefficients to allow these functions to exploit enough information for image classification. In the second part, starting with

the fuzzy membership degree of image pixels and the fuzzy dependence of image greyscale characteristics [16], mathematical models of attribute reduction information entropy are presented. Based on the constructed models, a reasonable interpretation of the characterized information on coal dust particulates is discussed [17]–[19]. The above works were carried out as theoretical and experimental verification for overlapping particulate separation research in advance, and they provide a basis for coal dust particulate recognition [20].

This paper is one part of the research "Denoising Mechanism and Image Recognition Research on Coal Dust Characteristic Parameters (51804249)". Through the analysis of coal dust particles, the physical properties of the dust are obtained, and an image characteristic model is established. The correlation between image parameters and coal dust characteristics is derived. A follow-up study on parameters such as particle size, particle size distribution, and coal dust concentration will be conducted. The research results of this paper can provide a theoretical and experimental basis for designing a detection system for coal dust explosions.

The remainder of this paper is organized as follows. In Section 2, the methods for the attribute reduction feature space model is introduced, and the approach of information entropy multi-attribute reduction for image extraction is presented. In Section 3, several experiments are presented to evaluate the performance of the proposed approach. Section 4 draws some conclusions and presents future works.

II. MATERIALS AND METHODS

A. REDUCTION OF DECISION INFORMATION SYSTEM

The experiment introduces the concept of a discernibility matrix into the analysis of coal dust image feature space and evaluates the fuzzy discernibility matrix of the fuzzy information system to determine all fuzzy attribute reductions. The feature selections based on the evaluated attribute reductions are the core issues of the redundant attribute removal in the image feature space. Assuming that $U = \{x_1, x_2, \dots, x_n\}$ is a finite nonempty set describing the n dimensional imagery feature space of coal dust, the binary group $FAS = (U, A \cup C)$ is the imagery fuzzy approximation space, where A is the fuzzy equivalence relation of U , and C is the single fuzzy decision attribute; $\forall x \in U$, the fuzzy equivalence class of the object x is

$$\mu_{[x]_A}(y) = \mu_A(x, y) \tag{1}$$

Assuming $U/A = \{A_1, A_2, \dots, A_K\}$, $U/C = \{C_1, C_2, \dots, C_l\}$, $\forall A_s \in U/A$ ($1 \leq s \leq k$), $\forall x \in U$, a fuzzy positive domain of C is

$$\begin{aligned} POS_A(C)(x) &= \mu_{POS_A(C)}(x) \\ &= \sup_{A_s \in U/A} \min \{ \mu_{A_s}(x), \mu_{POS_A(C)}(A_s) \} \end{aligned} \tag{2}$$

In the fuzzy approximation space $FAS = (U, A \cup C)$, $A_0 \subset A$, then A_0 is a fuzzy attribute reduction of A relative to C .

A sample coal dust image is set as an object, various coal dust features are set as conditional attributes, category results are set as decision attributes, and then, a decision table is formed. The essence of the process of extracting effective features is the attribute reduction process in the decision table. The decision table obtained by discretization can be used as a set of formulas processed with a logical relation, and the consistency of the decision table can be determined by judging whether the formulas and rules are contradictory. Attribute reduction is exactly based on the consistency of the decision table [21].

Important image information features such as colour, shape, texture, and spatial position of the object or region are analysed and retrieved to obtain effective imagery information and conduct image recognition. The selection of image features is performed by trial and error. Under the principle of classification accuracy based on the maximum likelihood method, six classification features selected from more than ten features are determined as items of effective feature information sensitive to extraction accuracy. First, we set six characteristic information elements, including the greyscale mean value, greyscale variance, contrast, mean texture, roughness, and evenness, to represent condition attribute A . Second, these characteristic information elements are continuous values, discretization is carried out by using the minimum description length principle algorithm, and thus, a decision table is generated. Finally, by acquiring effective feature information, the target category attribute, namely, decision attribute C , is determined to accomplish image recognition.

B. ATTRIBUTE REDUCTION ALGORITHM DESCRIPTION

The attribute reduction of the decision table can be realized with the following algorithm.

1) INPUT

Decision table $T = \{U, A \cup C, V, f\}$, where U is the universe of discourse, and A and C are the conditional attribute set and decision attribute set, respectively.

2) OUTPUT

Relative attribute reduction of the decision table.

3) ALGORITHM PROCESS

(1) Assume that dx is the decision rule, and the constraints of dx to A and C are described as $dx|A(\text{condition})$ and $dx|C(\text{decision})$, respectively.

① If $y \neq x$, for any decision rule, suppose $dx|A = dy|A$ and $dx|C = dy|C$; then the decision table is consistent;

② If $y \neq x$, $\exists dx|A = dy|A$, while $dx|C \neq dy|C$, then the decision table is inconsistent. Calculate its positive region $POS(A, C)$.

(2) If $r \in A$, and $\text{ind}(A) = \text{ind}(A - \{r\})$, then r is a redundant attribute, which can be omitted. Otherwise, reserve it.

(3) If $r \in A$, $POS(A, C) = POSX(A - \{r\}, C)$ is true, then r can be omitted. Otherwise, reserve it.

(4) Finally, a decision table $T_0 = \{U, A_0 \cup C, V_0, f\}$ is derived, where $A_0 \subset A$, A_0 is the relative reduced attribute set of A , and this contains the effective feature set.

A small part of the condition attribute was omitted through the analysis of data, and objects with the same decision rules were merged in the decision table. Thus, the reduced decision table could be obtained, and effective feature information could be determined. The essence of the process is the attribute reduction in the decision table.

Through simplification of the condition attributes in the decision table, the simplified decision table had the same function as that in the previous one, but the number of condition attributes was decreased. The same decision could be implemented based on fewer conditions, and this is the purpose of attribute reduction [22]. The simplified decision table is incomplete. It contains only the necessary condition attribute values, but it has all the information of the original information system.

C. DETERMINING THE FUZZY CATEGORY MEMBERSHIP

Image pixels can be described with the feature space points of the information system obtained by attribute reduction. Image extraction can be considered an object classification problem, and the dust images can be extracted by feature space clustering. This procedure will obtain the aggregation extraction characteristic in the feature space, which is then mapped back to the original image space. Thus, the optimal extraction effect can be determined.

If U is the reference superset, R is the equivalent relationship on U , and X is a subset of U , then X is said to be a fuzzy subset of U if $X = \{x, \mu_X(x)\}, \forall x \in U$.

Supposing

$$\underline{R}(X) = \{x_i | [x_i]_R \subseteq X\} \tag{3}$$

$$\overline{R}(X) = \{x_i | [x_i]_R \cap X \neq \emptyset\} \tag{4}$$

Then, $\underline{R}(X)$ is called the lower approximation of R and $\overline{R}(X)$ the upper approximation of R . If $\underline{R}(X) = \overline{R}(X)$, X is called a definable set, otherwise it is called a rough set.

The coal dust images obtained were treated as fuzzy rough set $X = \{x_1, x_2, \dots, x_n\}$. From the perspective of indistinguishable relations and classes, k clusters $\{m_1, m_2, \dots, m_k\}$ were constructed in the fuzzy rough sets $X = \{x_1, x_2, \dots, x_n\}$, and the simplified and general rules were obtained from a large volume of original data. Thus the fuzzy membership degree $\mu_{wi(x_i)}$ of x_i corresponding to wi was determined, where x_i is the gray value of the i pixel in the coal dust image; $i = 1, 2, \dots, n$; n is the number of pixel points, k is the non-zero natural number, and wi is the pixel in the universe of discourse of the fuzzy rough set U .

D. ACHIEVING THE FUZZY ATTRIBUTE REDUCTION OF FUZZY ROUGH SET

When coal dust features were extracted from an image information system, redundant information easily existed in the extracted features according to the importance of the image

feature information. The attribute reduction could be adopted by simplification of the classification standards, elimination of the redundant feature information, and selection of the most important extraction features [23].

In the gray feature space of the coal dust image, multiple image gray features were treated as multiple condition attributes, and the fuzzy dependence $\gamma_x(A_\gamma)$ of condition attributes A_γ was obtained according to the following formula:

$$\gamma_X(A_r) = \frac{|\text{POS}_X(A_r)|}{|U|} \quad (5)$$

where $\text{POS}_X(A_\gamma)$ is the positive domain of the fuzzy rough set X corresponding to condition attributes A_γ . The formula is as follows:

$$\text{POS}_X(A_r) = \sup \min \{ \mu_{w_i}(x_i), \mu_{\text{POS}_X(A_r)}(x_i) \} \quad (6)$$

where $\mu_{\text{POS}_X(A_\gamma)}(x_i)$ is the fuzzy category membership of x_i corresponding to $\text{POS}_X(A_\gamma)$:

$$\mu_{\text{POS}_X(A_r)}(x_i) = \begin{cases} \frac{x_i - m_j}{m_{j-1} - m_j} & m_{j-1} \leq x_i \leq m_j \\ \frac{x_i - m_j}{m_{j+1} - m_j} & m_j \leq x_i \leq m_{j+1} \\ 0 & \text{else} \end{cases} \quad (7)$$

By examining the fuzzy dependencies corresponding to N condition attributes in the gray feature space of the coal dust images, the condition attribute with the maximum fuzzy dependence was selected from $\{A_1, A_2, \dots, A_N\}$ as the candidate attribute of fuzzy attribute reduction, defined as A'_1 . According to the above method, the candidate attributes of the $2 - \lambda$ fuzzy attribute reductions were determined in turn, and defined as the candidate attribute set $B = \{A'_1, A'_2, \dots, A'_q\}$ of the fuzzy attribute reduction. Here, the candidate attribute A'_q of the fuzzy attribute reduction was the conditional attribute of the maximum fuzzy dependence with the exception of the selected candidate attribute $q - 1$, and the range of q is $[2, \lambda]$.

The images of coal dust inevitably had feature redundancies. To address the problem of redundant features, attribute selection was carried out according to the classification importance and attribute reduction of the fuzzy rough set. The attributes with the greatest importance were selected and retained, while redundant attributes A_v ($q < v < N$) were removed. It was assumed that this relationship was true, where A_v is the fuzzy dependence, which is greater than that of other candidate attributes of fuzzy attribute reductions. Then $B' = \{A'_1, A'_2, \dots, A'_q, A_v\}$ was determined to be the fuzzy attribute reduction of the fuzzy rough set, and the image with redundant attributes removed could be obtained. Otherwise, $B = \{A'_1, A'_2, \dots, A'_q\}$ was determined to be the fuzzy attribute reduction of the fuzzy rough set X , and the image with redundant attributes removed was obtained.

E. ANALYSIS OF INFORMATION ENTROPY CHARACTERISTICS OF COAL DUST IMAGE

Assume that the initial extraction threshold s of the coal dust image was

$$s = [x_{\min} + \frac{1}{2}(x_{\max} - x_{\min})] \times \text{rand}() \quad (8)$$

and each pixel gray value of the coal dust image was compared with extraction threshold s . Here, x_{\max} is the maximum value of elements of x as follows:

$$x_{\max} = \max \{x_1, x_2, \dots, x_n\} \quad (9)$$

x_{\min} is the minimum value of elements of x as follows:

$$x_{\min} = \min \{x_1, x_2, \dots, x_n\} \quad (10)$$

and $\text{rand}()$ is the random number distributed uniformly on $(0,1)$.

Due to the fuzzy uncertainty of the boundary between the object and background in the coal dust grayscale image, the upper and lower approximations of rough sets can be adopted to describe this uncertainty. For the coal dust image with redundant attributes removed, this study applied the fuzzy upper approximation and fuzzy lower approximation to the object region and background region, which are given as follows:

Fuzzy lower approximation of object region:

$$\underline{R}_{oX} = \inf_{x_i \in U} \max \{1 - \mu_{w_i}(x_i), w_i > s, \} \quad (\exists i = 1, 2, \dots, n) \quad (11)$$

Fuzzy upper approximation of object region:

$$\overline{R}_{oX} = \sup_{x_i \in U} \min \{ \mu_{w_i}(x_i), w_i \leq s, \} \quad (\forall i = 1, 2, \dots, n) \quad (12)$$

Fuzzy lower approximation of background region:

$$\underline{R}_{bX} = \inf_{x_i \in U} \max \{ \mu_{w_i}(x_i), w_i > s, \} \quad (\exists i = 1, 2, \dots, n) \quad (13)$$

Fuzzy upper approximation of background region:

$$\overline{R}_{bX} = \sup_{x_i \in U} \min \{ \mu_{w_i}(x_i), w_i \leq s, \} \quad (\forall i = 1, 2, \dots, n) \quad (14)$$

When each pixel gray value of the coal dust image is more than the extraction threshold s , the fuzzy lower approximation of the object region is $\underline{R}_{oX} + 1$. When a part of the pixels' grey values is more than the extraction threshold s , the fuzzy upper approximation of the object region is $\overline{R}_{oX} + 1$. When each pixel grey value of the coal dust image is no more than the extraction threshold s , the fuzzy lower approximation of the background region is $\underline{R}_{bX} + 1$. When a part of the pixels' grey values is no more than the extraction threshold s , the fuzzy upper approximation of the background region is $\overline{R}_{bX} + 1$.

The information measure and acquisition limitation of the coal dust image feature could easily result in information discontinuity, and thus information granules were formed. Discrete data points in the information granules were taken as a whole to measure knowledge uncertainty in the information system. In the range of entropy space, the universe

of discourse could be divided by the granularity similarity and inferred from the subset. During information processing, information granules had different amounts of information, and the uncertainty degree of the information system could be described by information entropy. The higher the information entropy was, the more uncertain the system became and thus the greater amount of information to be determined was required.

Given the universe of discourse U , suppose that P is an information granule of U , and its derived partition on U is $U/P = \{X_1, X_2, \dots, X_n\}$, Let

$$p(X_i) = \frac{|X_i|}{|U|} \quad (15)$$

then, the entropy of information granules $\text{Entr}(P)$ is as follows:

$$\text{Entr}(P) = - \sum_{i=1}^n p(X_i) \log_2 p(X_i) \quad (16)$$

The Hartley metric expression of information entropy of the universe of discourse U was the knowledge entropy. Based on the information theory principle, the information entropy of certain knowledge was subtracted from the Hartley metric of U , and thus, rough entropy of the knowledge was obtained.

The knowledge rough entropy $H_r(P)$ was defined as a partition of a universe with an equivalence relation, and the general binary relationship obtained by extending the equivalence relation to a compatible relationship or a similar relationship was considered. The frequency of occurrence of any object in the neighbourhood of all objects constructed with the general binary relationship could determine the knowledge rough entropy $H_r(P)$, and the formula is written as

$$H_r(P) = \frac{1}{|U|} \sum_{i=1}^{|U|} \log_2 |X_i|_P \quad (17)$$

where $U = \{x_1, x_2, \dots, x_{|U|}\}$, $P \subseteq A$,

$$|X_i|_P = |\{P(X_j) | X_i \in P(X_j), 1 \leq j \leq |U|\}| \quad (18)$$

namely, the frequency of occurrence of X_i in the neighbourhood of all elements X_j ($1 \leq j \leq |U|$). $P(X_j)$ represents the neighborhood of X_j constructed with a general binary relationship under knowledge P .

Obtaining more accurate uncertain measurement characteristics of rough sets in coal dust images is related not only to the uncertainty of universe knowledge (rough entropy of knowledge) but also to the roughness of rough sets. Thus, the rough entropy model of a rough set could be established.

Given the information system $S = (U, A)$, $P \subseteq A$, $X \subseteq U$, the rough entropy of a rough set under the knowledge P is defined as follows:

$$H_r(P) = \rho_P(X) H_r(P) \quad (19)$$

where, $\rho_P(X)$ is the roughness under the knowledge P , defined as follows:

$$\rho_P(X) = 1 - \frac{|P_-(X)|}{|P^-(X)|} \quad (20)$$

where $P_-(X)$ and $P^-(X)$ denote the lower and upper approximation sets about the knowledge P under the general binary relationship, respectively.

Based on the discussion above, within the scope of entropy space, a quantitative model could be established using the concept of information entropy. From the perspective of set theory and algebra analysis, based on the definition of image roughness, the rough information entropy is as follows:

$$\text{Entr}(X) = (1 - \underline{R}_{oX}) \log_2 \bar{R}_{oX} + (1 - \underline{R}_{BX}) \log_2 \bar{R}_{BX} \quad (21)$$

The information entropy of coal dust image $\text{Entr}(X)$ was determined, the maximum entropy was finally obtained, and the selection of the coal dust image extraction threshold was achieved.

III. RESULTS AND DISCUSSION

To investigate the segmentation performance, a series of experiments was carried out based on coal dust samples. In this experiment, the fuzzy category membership degrees could be calculated by labelling each pixel in several dust images with some well-defined multi-segment function labels in a patch-wise manner. As the fuzzy attribute reduction could be extracted step by step, the fuzzy lower approximation and upper approximation in the target and background regions were divided naturally. Thus, the information entropy model of coal dust particulates was established. In this section, two experiments were carried out to evaluate the performance of the proposed approach for IEMAR image segmentation, which are listed as follows.

(1) In the first experiment, 30 image sets were utilized to evaluate the extraction performance of the learned discriminative features.

(2) Second, performance parameter data sets that evaluate image extraction accuracy were employed to verify the effectiveness of the proposed approach by comparison with other conventional segmentation approaches.

A. PERFORMANCE EVALUATION OF PARTICULATE IMAGE FEATURE

1) DATASET AND PARAMETER SETTING

To verify the rationality of the information entropy multi-attribute reduction model and evaluate the performance of the proposed method, 30 groups of image sets (35 pictures were taken for each group) with different sizes were utilized in this experiment. The coal sample datasets were taken from a coal preparation plant. The sampling standard was performed according to the « Manual methods for ambient air quality monitoring » (HJ194-2017). Twelve dust sampling locations were selected in multiple dust production workshops of the coal preparation plant. The acquired 30 groups of training samples were classified by the different conditions of sampling image light source, sampling image time interval, and sampling image temperature. The image characteristics of coal dust with differing particle sizes were identified. Due to limited space, only some samples are listed and shown here. In the computing environment of a Pentium Dual Core G3420

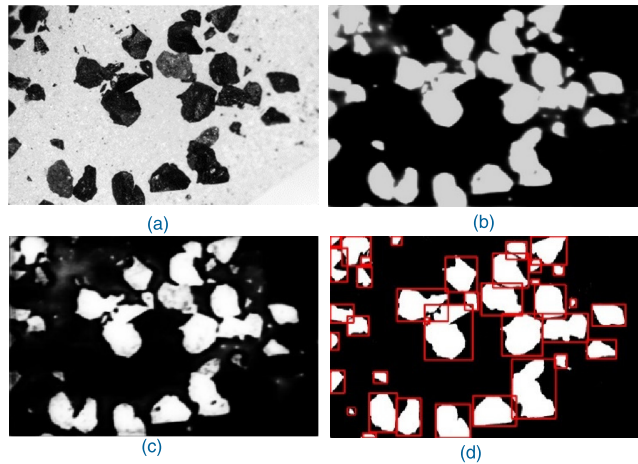


FIGURE 1. Comparison of different approaches of particle size $\geq 200 \mu\text{m}$: (a) original image, (b) FPM, (c) SFC, and (d) IEMAR.

CPU 4GB RAM PC, images were acquired using Olympus BX41 (microscopic magnification factors: $40\times$ ocular lens, $10\times$ objective lens) and MATLAB 2018. Insufficient training samples easily cause experimental results to fluctuate severely by random sampling, while the experimental results obtained by cross validation are relatively stable. Therefore, cross-validation methods are considered. The specific steps are as follows: randomly sample 30 groups with 35 images in each group, divide the image sets randomly and complete 10 experiments. A set of images is taken as the sample test set for each experiment, and the remaining sets are taken as the training sets. Finally, the arithmetic means of 10 experiments are taken as the final result.

In this experiment, particulate images (Figs. 1-3), which were acquired in mine preparation plants, were used to evaluate the discriminative capacity of the proposed approach. Objects of the experiment were taken from coal dust images of different particle sizes, and each of the raw datasets was 3072×1048 pixels in size.

2) ANALYSIS OF RESULTS

Based on the good performance in terms of sensitivity and specificity, two representative approaches are introduced here: feature-point matching (FPM) [24] and spatial fuzzy clustering (SFC) [25] for comparison with the IEMAR. The coal dust images with particle sizes $\geq 200 \mu\text{m}$, $75 \mu\text{m} \leq$ particle sizes $< 200 \mu\text{m}$, and particle sizes $< 75 \mu\text{m}$ are shown in Figs. 1-3 (a), respectively. the extraction results are shown in Figs. 1-3 (b), (c), and (d).

Based on the analysis of the above experimental results, for image objects with slightly different grey values, the model algorithm based on FPM did not have an obvious extraction effect on the image feature information and thus easily resulted in great loss of image information. The SFC model algorithm not only considered the spatial characteristics but also processed the pixel grey values; thus, it is relatively sensitive to noise and has good information extraction ability. However, the ability to distinguish information is weak in the

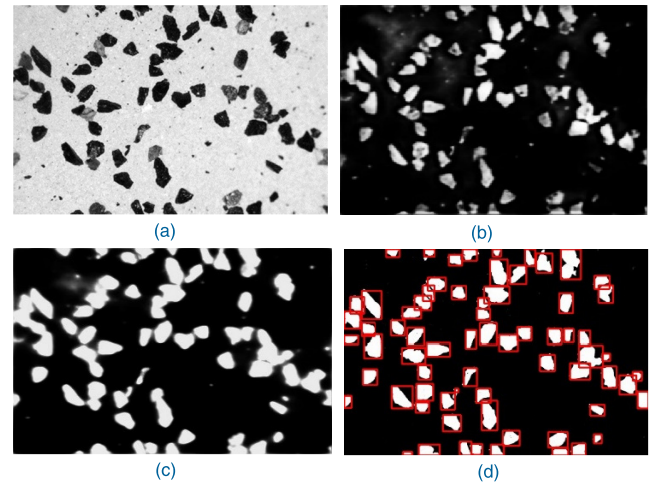


FIGURE 2. Comparison of different approaches of $75 \leq$ particle size $< 200 \mu\text{m}$: (a) original image, (b) FPM, (c) SFC and (d) IEMAR.

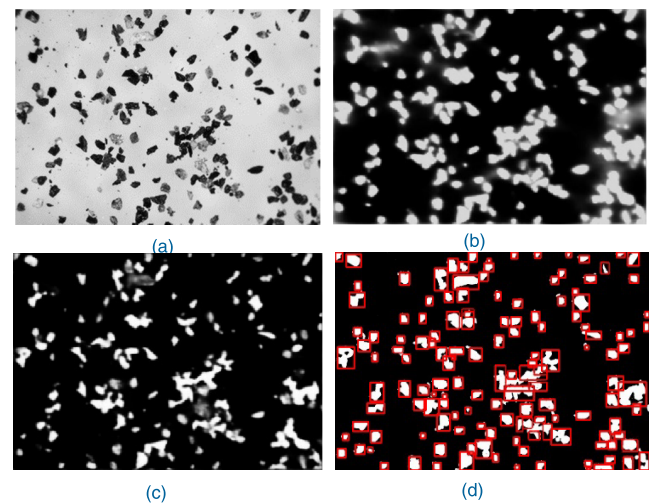


FIGURE 3. Comparison of different approaches for particle size $< 75 \mu\text{m}$: (a) original image, (b) FPM, (c) SFC, and (d) IEMAR.

overlapping regions of grey values. At the same time, it can also be noticed the performance is effectively improved by introducing the discriminative information of multi-attribute reduction after comparing the statistical results between SFC and the proposed IEMAR. The established IEMAR model has a good degree of discrimination for detailed image information. Compared with the statistical results of IEMAR, the high-level features that were extracted by the information entropy structure can effectively characterize the content of image sets. This method can better identify the most important feature information used for extraction, particularly for smaller particulates, and can also accurately extract particulates from images. also extract particulates from images accurately.

B. DISCUSSION

1) PARAMETERS ANALYSIS

The performance indexes used to evaluate the discriminative features of the particulate image region are represented as the

TABLE 1. Differences in performance test parameters for three particle sizes ranges. Optimal threshold, computational time (s) and unclassified rate evaluation are listed for the nine different treatments. Optimal performance value indicated in bold. All parameters mean values were measured at the end of the test.

Particle size	Performance indices	Approaches								
		MSIA	DWT	FHH	GLCM	FCM	Gabor	FPM	SFC	IEMAR
$\geq 200 \mu\text{m}$	Optimal threshold	142.3	135.8	167.5	159.2	125.6	138.9	156.6	142.4	134.6
	Computational time (s)	11.42	12.35	10.89	13.24	10.25	10.28	8.86	9.01	9.03
	α	0.658	0.746	0.854	0.679	0.865	0.886	0.835	0.923	0.978
$75 \leq \text{particle size} < 200 \mu\text{m}$	Optimal threshold	146.5	142.9	175.2	168.4	141.0	146.7	164.6	154.3	138.5
	Computational time (s)	13.24	14.52	11.99	13.56	11.84	11.20	9.24	9.16	9.26
	α	0.610	0.710	0.811	0.688	0.753	0.821	0.768	0.847	0.958
$< 75 \mu\text{m}$	Optimal threshold	156.7	151.8	185.4	177.2	152.6	153.9	159.3	151.1	140.3
	Computational time (s)	13.25	15.89	12.52	14.23	12.99	12.95	9.47	9.39	9.57
	α	0.548	0.598	0.753	0.621	0.724	0.754	0.698	0.867	0.950

optimal threshold, computational time, and unclassified rate evaluation. In this section, the above three parameters were used to evaluate the performance of the proposed approach for image extraction. To verify the performance of the optimal threshold, computational time, and unclassified rate evaluation for the characteristic parameters of a coal dust image, several approaches that are widely used to process particulate images were compared by using images of different particle sizes: multiscale image acquisition (MSIA) [26], Daubechies wavelet transform (DWT) [27], Frenkel-Halsey-Hill (FHH) [28], grey-level cooccurrence matrix (GLCM) [29], fuzzy C-means (FCM) [9], Gabor filter [30], FPM, and SFC. In the process of testing the simulations with the approaches in the above works, the adopted test conditions, such as temperature, humidity, light intensity, coal dust sample specifications and other parameters, are not the same, so the measured indexes are different. This paper focuses on the comparative analysis of the identification accuracy of coal dust particulate samples under their respective conditions.

Experimental objects were taken from the coal dust image with differing particle sizes collected from some coal mine preparation plants in the environment of Pentium Dual Core G3420 CPU 4GB RAM PC, Olympus BX41, and MATLAB 2018 software. More specifically, to provide a fair comparison, we used the same parameter settings and input datasets in our evaluation test. Three performance indices for coal dust images with differing particle sizes are listed in Table 1: optimal threshold, computational time (s), and unclassified rate evaluation α . The unclassified rate evaluation is defined as follows:

$$\alpha = 1 - \beta \quad (22)$$

$$\beta = \frac{2t \sum_{j=0}^t \sum_{i \in Z_j} (g_i - \bar{g}_j)^2}{x \cdot y \cdot (R_{\max} - R_{\min})^2} \quad (23)$$

where g_j is the grey value of pixel i , \bar{g}_j is the average grey value of the j th order segmentation region, Z_j is the j th order segmentation region, t is the number of thresholds, $x \cdot y$ is the total number of image pixels, and R_{\max} and R_{\min} are the maximum and minimum grey values of the image, respectively. The range of parameter α is $[0, 1]$. The closer the value of α is to 1, the greater the image extraction accuracy and the better the extraction effect.

The difference in performance between the proposed IEMAR and the others was analysed by sequential extraction (Table 1). The results show that IEMAR achieves an unclassified rate evaluation α value above 0.95 to resolve the unclear characteristic mode. When MSIA, DWT, FHH, GLCM, FCM, Gabor filter, FPM, and SFC were compared, only FPM and SFC were slightly faster than IEMAR in terms of computation time, but the α values of the two approaches were 0.835 and 0.923, respectively, which are worse than that of the proposed IEMAR. Meanwhile, the bold fonts in Table 1 are employed to denote the optimal results, which occurs in the situation in which IEMAR outperforms the others. Although IEMAR was associated with only less fuzzy feature information, it still achieved improved accuracy and efficiency. Precisely because of the approach of combining fuzziness and roughness in information systems with product fuzzy classification rules, IEMAR results in strengthened generalization ability. In summary, IEMAR achieves the best trade-off between accuracy and speed. Utilizing IEMAR can improve the search efficiency, and it guarantees the

effectiveness and robustness of the image extraction approach to a greater degree.

Considering the balance of extraction accuracy and computational efficiency, IEMAR is a practical and effective image extraction algorithm. The threshold value, computational time and α have significant advantages and meet the requirements of an accurate extraction. IEMAR can also provide accurate data for follow-up studies of coal dust image information.

2) DISCRIMINATIVE CAPACITY ANALYSIS

In this section, three simulation experiments were conducted to evaluate the performance of the proposed IEMAR with respect to different settings. Conventional test methods consist of cross validation and random sampling. The insufficient training samples make the experimental results of random sampling fluctuate greatly, while the experimental results obtained by cross validation are relatively stable. Therefore, cross validation is applied here. the specified operation is as follows.

(1) The particulate ranges were determined in the particle sizes of $0 \sim 75 \mu\text{m}$, $75 \sim 200 \mu\text{m}$, and $\geq 200 \mu\text{m}$;

(2) Thirty groups of image sets were sampled, including 35 random image samples in each group, and they were utilized to achieve ten experiments;

(3) A group of image sets was set as the sample test set for each experiment, while the others were taken as training sets. Finally, the arithmetic mean values of ten experiments were considered as the final result.

As a result, the parameters of all samples were analysed, and the results are shown in Fig. 4(a) - (c).

The threshold parameter means of these dust image sets with different particle sizes are listed in Fig. 4(a) after 10 runs. It can be observed that low thresholds could be achieved by DWT, FCM and the proposed IEMAR on all of these image sets. Meanwhile, from the discriminative sensitivity and computational accuracies of the algorithm, it can be observed that the three approaches, i.e., DWT, FCM and IEMAR, performed better than all other six approaches in the vast majority of cases. However, from an overall point of view, the IEMAR approach had a low threshold, especially for dust particle sizes $< 75 \mu\text{m}$. When enough training samples were included, the highest average extraction accuracy of the proposed approach was reached on the datasets with various particle sizes. This result also means that IEMAR may be a better choice when extracting the specified low greyscale image.

Fig. 4(b) also shows that the computational time appeared much better on IEMAR, FPM and SFC, which had values of 9.03, 8.86, and 9.01 for particle sizes $\geq 200 \mu\text{m}$, 9.26, 9.16, and 9.14 for particle sizes in the range of $[75 \mu\text{m}, 200 \mu\text{m}]$ and 9.57, 9.47, and 9.39 for particle sizes $< 75 \mu\text{m}$, respectively. This result means that the three approaches may be better choices when image extraction is conducted with different particle sizes. However, it can also be seen from the data sets in Table 1 that the FPM and SFC had fast

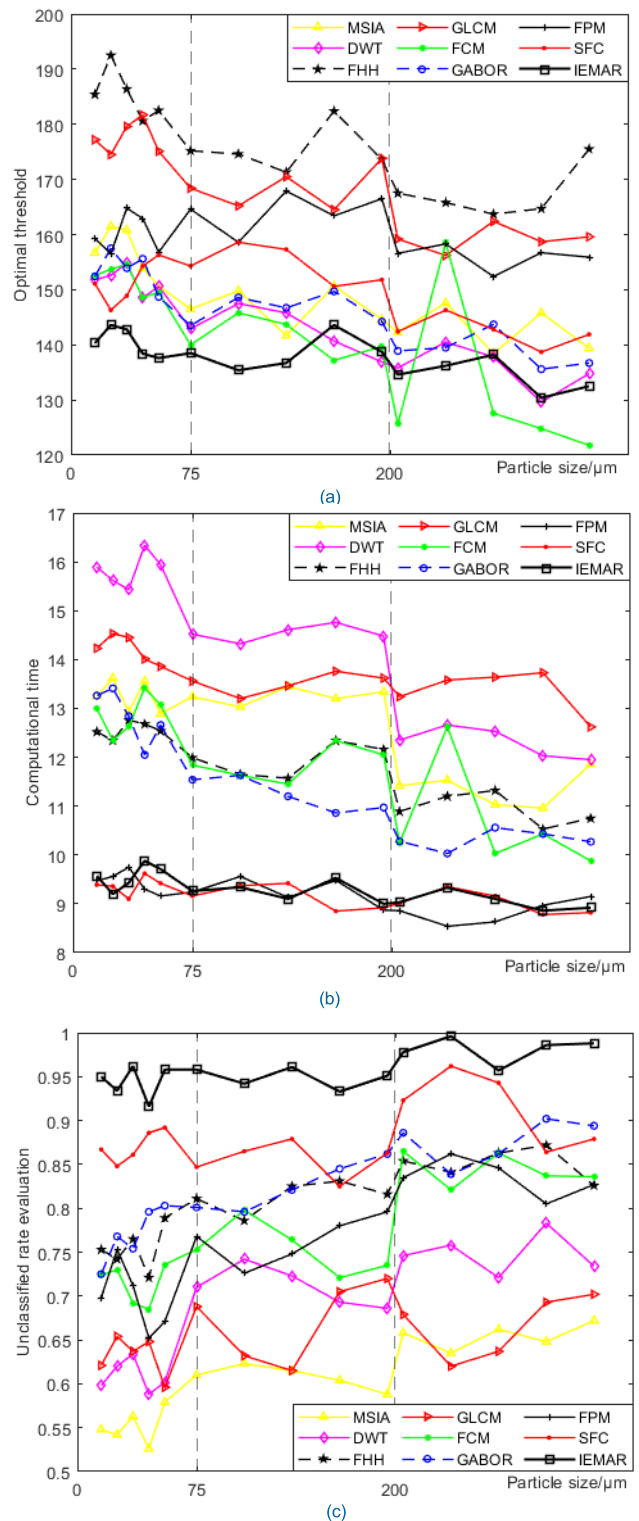


FIGURE 4. Performance comparison under different approaches treatments for (a) optimal Threshold, (b) computational time and (c) unclassified rate evaluation. The vertical dashed lines indicate the different particulate ranges division ($< 75 \mu\text{m}$, $[75 \mu\text{m}, 200 \mu\text{m})$, $\geq 200 \mu\text{m}$).

computational times, while the two other indicators were unstable, and the accuracies were lower than that of the IEMAR model. The above simulation test results are utilized

to evaluate the performance between the proposed IEMAR and all other methods. It is clear that IEMAR can achieve the highest accuracy while it correlates with less fuzzy feature information. This finding is mainly attributed to the fuzzy classification rules that have strong generalization ability, with which fuzziness is combined with the roughness of the information system.

Finally, the unclassified rate evaluation α mean for feature discrimination is also recorded and shown in Fig. 4(c). Along the whole horizontal axis, α of the feature information increased with the particle size of the image sets. When the particle size was $<75 \mu\text{m}$, the α of the MSIA model was 0.548, DWT was 0.598, FHH was 0.753, GLCM was 0.621, FCM was 0.724, GABOR was 0.754, FPM was 0.698, SFC was 0.867 and the α of the IEMAR model was 0.950. When the particle size was in the range $[75 \mu\text{m}, 200 \mu\text{m})$, the α of the MSIA model was 0.610, DWT was 0.710, FHH was 0.811, GLCM was 0.688, FCM was 0.753, GABOR was 0.821, FPM was 0.768, SFC was 0.847, and the α of the IEMAR model was 0.958. Finally, when the particle size was $\geq 200 \mu\text{m}$, the α of the proposed IEMAR was 0.978. The curve analysis in Fig. 4(c) shows that the α of IEMAR was above 0.95, which is significantly higher than the others. While the approaches with poor performance were susceptible to their own generated noises, they were relatively vague for low-grey image processing. Thus, these approaches had low accuracy in processing coal dust images with small particle sizes. Meanwhile, it can be observed that the difference in the unclassified evaluation determined by IEMAR over the whole particle size range is not clear. The high-level discriminative features obtained by the proposed IEMAR approach reach the highest value compared with the others. This result indicates that enough discriminant information could be captured by IEMAR, which is essential for particulate image extraction. In summary, it can be observed that the IEMAR model exhibits good discrimination ability for image detail area information, which can identify the important feature information. This finding ensures accurate results for coal dust images with various particle sizes by extracting fewer feature values.

IV. CONCLUSION

In this study, we proposed a hierarchical information division approach for the characterizing the spatial image characteristics using IEMAR computing. The most distinguishing feature of the proposed algorithm is that IEMAR achieves the best trade-off between accuracy and computing speed. This approach consists of two-fold outperformances: 1) the attribute reduction model reduces the impact of the loss of continuous data attribute information due to disappearance of the attribute ordered structure, which can reduce the information loss to some extent; and 2) the established information entropy model can delete the redundant attributes and select the most important classification attributes. The proposed approach yielded a significant performance improvement and computed the unclassified rate evaluation correspondences

with an average of 0.950 even for particle sizes $< 75 \mu\text{m}$ for a sequence of 30 sets of images to resolve the unclear characteristic mode.

REFERENCES

- [1] N. Lilić, I. Obradović, and A. Cvjetić, "An intelligent hybrid system for surface coal mine safety analysis," *Eng. Appl. Artif. Intell.*, vol. 23, no. 4, pp. 453–462, Jun. 2010.
- [2] W. Du, Y. Levin-Schwartz, G.-S. Fu, S. Ma, V. D. Calhoun, and T. Adali, "The role of diversity in complex ICA algorithms for fMRI analysis," *J. Neurosci. Methods*, vol. 264, pp. 129–135, May 2016.
- [3] Z. Zhang, J. Yang, Y. Wang, D. Dou, and W. Xia, "Ash content prediction of coarse coal by image analysis and GA-SVM," *Powder Technol.*, vol. 268, pp. 429–435, Dec. 2014.
- [4] O. S. Agimelen, A. J. Mulholland, and J. Sefcik, "Modelling of artefacts in estimations of particle size of needle-like particles from laser diffraction measurements," *Chem. Eng. Sci.*, vol. 158, pp. 445–452, Feb. 2017.
- [5] J.-P. Sun, W. Chen, F.-Y. Ma, F.-Z. Wang, L. Tang, and Y.-J. Liu, "Classification of infrared monitor images of coal using an feature texture statistics and improved BP network," *J. China Univ. Mining Technol.*, vol. 17, no. 4, pp. 489–493, Dec. 2007.
- [6] X.-M. Ma, "A revised edge detection algorithm based on wavelet transform for coal gangue image," in *Proc. Int. Conf. Mach. Learn. Cybern.*, Aug. 2007, pp. 1639–1642.
- [7] Alpana and S. Mohapatra, "Machine learning approach for automated coal characterization using scanned electron microscopic images," *Comput. Ind.*, vol. 75, pp. 35–45, Jan. 2016.
- [8] O. Rahmati, M. Panahi, S. S. Ghiasi, R. C. Deo, J. P. Tiefenbacher, B. Pradhan, A. Jahani, H. Goshtasb, A. Kornejady, H. Shahabi, A. Shirzadi, H. Khosravi, D. D. Moghaddam, M. Mohtashamian, and D. T. Bui, "Hybridized neural fuzzy ensembles for dust source modeling and prediction," *Atmos. Environ.*, vol. 224, Mar. 2020, Art. no. 117320.
- [9] W. William, A. Ware, A. H. Basaza-Ejiri, and J. Obungoloch, "Cervical cancer classification from pap-smears using an enhanced fuzzy C-means algorithm," *Informat. Med. Unlocked*, vol. 14, pp. 23–33, Jan. 2019.
- [10] H. Guo, B. Su, Z. Bai, J. Zhang, and X. Li, "Novel recognition method of blast furnace dust composition by multifeature analysis based on comprehensive image-processing techniques," *JOM*, vol. 66, no. 11, pp. 2377–2389, Nov. 2014.
- [11] H. Pan, W. Mi. (2019). *An Adaptive Decoder Design Based on the Receding Horizon Optimization in BMI System*, *Cognit. Neurodyn*, doi: [10.1007/s11571-019-09567-4](https://doi.org/10.1007/s11571-019-09567-4).
- [12] J. Sun and B. Su, "Coal-rock interface detection on the basis of image texture features," *Int. J. Mining Sci. Technol.*, vol. 23, no. 5, pp. 681–687, Sep. 2013.
- [13] H. Pan, W. Mi, X. Lei, J. Deng, "A closed-loop brain-machine interface framework design for motor rehabilitation," *Biomed. Signal Process. Control*, vol. 58, Apr. 2020, Art. no. 101877, doi: [10.1016/j.bspc.2020.101877](https://doi.org/10.1016/j.bspc.2020.101877).
- [14] M. Wei, M. Tong, J. Hao, L. Cai, and J. Xu, "Detection of coal dust in a mine using optical tomography," *Int. J. Mining Sci. Technol.*, vol. 22, no. 4, pp. 523–527, Jul. 2012.
- [15] F.-Y. Ma and S. Song, "Improved algorithm of pattern classification and recognition applied in a coal dust sensor," *J. China Univ. Mining Technol.*, vol. 17, no. 2, pp. 168–171, Jun. 2007.
- [16] H.-Y. Yu, X.-B. Zhi, and J.-L. Fan, "Image segmentation based on weak fuzzy partition entropy," *Neurocomputing*, vol. 168, pp. 994–1010, Nov. 2015.
- [17] Y. Lin, Y. Li, C. Wang, and J. Chen, "Attribute reduction for multi-label learning with fuzzy rough set," *Knowl.-Based Syst.*, vol. 152, pp. 51–61, Jul. 2018.
- [18] H. Li, D. Li, Y. Zhai, S. Wang, and J. Zhang, "A novel attribute reduction approach for multi-label data based on rough set theory," *Inf. Sci.*, vols. 367–368, pp. 827–847, Nov. 2016.
- [19] H. Yaghoobi, H. Mansouri, M. A. Ebrahimi Farsangi, and H. Nezamabadi-Pour, "Determining the fragmented rock size distribution using textural feature extraction of images," *Powder Technol.*, vol. 342, pp. 630–641, Jan. 2019.
- [20] L. Si, Z. Wang, C. Tan, and X. Liu, "A novel approach for coal seam terrain prediction through information fusion of improved D-S evidence theory and neural network," *Measurement*, vol. 54, pp. 140–151, Aug. 2014.

- [21] D. Wu and S. Zhang, "Research on image enhancement algorithm of coal mine dust," in *Proc. Int. Conf. Sensor Netw. Signal Process. (SNSP)*, Xi'an, China, Oct. 2018, pp. 261–265.
- [22] B. Zhou, P. Hatherly, and W. Sun, "Enhancing the detection of small coal structures by seismic diffraction imaging," *Int. J. Coal Geol.*, vol. 178, pp. 1–12, Jun. 2017.
- [23] F. Garcia-Lamont, J. Cervantes, A. López, and L. Rodriguez, "Segmentation of images by color features: A survey," *Neurocomputing*, vol. 292, pp. 1–27, May 2018.
- [24] Y. Yang, T. Ma, and S. Du, "Robust template matching with angle location using dynamic feature pairs updating," *Appl. Soft Comput.*, vol. 85, Dec. 2019, Art. no. 105804.
- [25] T. Li, Z. Jiang, Y. Rao, and X. Zhang, "Image segmentation based on gene expression programming and spatial fuzzy clustering," *J. Image Graph.*, vol. 22, no. 5, pp. 575–583, 2017.
- [26] R. Singh, N. Schwarz, N. Taesombut, D. Lee, B. Jeong, L. Renambot, A. W. Lin, R. West, H. Otsuka, S. Naito, S. T. Peltier, M. E. Martone, K. Nozaki, J. Leigh, and M. H. Ellisman, "Real-time multi-scale brain data acquisition, assembly, and analysis using an end-to-end OptIPuter," *Future Gener. Comput. Syst.*, vol. 22, no. 8, pp. 1032–1039, Oct. 2006.
- [27] A. Khare, M. Khare, Y. Jeong, H. Kim, and M. Jeon, "Despeckling of medical ultrasound images using daubechies complex wavelet transform," *Signal Process.*, vol. 90, no. 2, pp. 428–439, Feb. 2010.
- [28] A. L. Ahmad and N. N. N. Mustafa, "Pore surface fractal analysis of palladium-alumina ceramic membrane using Frenkel–Halsey–Hill (FHH) model," *J. Colloid Interface Sci.*, vol. 301, no. 2, pp. 575–584, Sep. 2006.
- [29] N. Rajkovic, J. Ciric, N. Milosevic, and J. Saponjic, "Novel application of the gray-level co-occurrence matrix analysis in the parvalbumin stained hippocampal gyrus dentatus in distinct rat models of Parkinson's disease," *Comput. Biol. Med.*, vol. 115, Dec. 2019, Art. no. 103482.
- [30] G. Srivastava and R. Srivastava, "Salient object detection using background subtraction, Gabor filters, objectness and minimum directional backgroundness," *J. Vis. Commun. Image Represent.*, vol. 62, pp. 330–339, Jul. 2019.



ZHENG WANG was born in Xi'an, China. She received the Ph.D. degree from the Xi'an University of Science and Technology, in 2016. From 2018 to 2019, she was a Visiting Scholar in image computation research with Xi'an Jiaotong University. Her research interests include image analysis and visualization, pattern recognition, and information extraction. She was a recipient of the National Natural Science Foundation of China, in 2018.



XU ZHENG received the M.S. degree from the Xinjiang Technical Institute of Physics and Chemistry, CAS, in 2004. She currently works with the Shaanxi Institute of Food and Drug Control. She had been engaged in drug inspection. Her research interests include drug quality analysis, drug safety evaluation, new drug pharmacodynamics evaluation, and other related work.



HONGGUANG PAN received the Ph.D. degree from Xi'an Jiaotong University, in 2015. From September 2013 to March 2016, he was a Visiting Ph.D. Student with Lehigh University, USA. He is currently a Lecturer with the Xi'an University of Science and Technology. His research interests include predictive control, brain-machine interface, and so on.



DONGYAN LI was born in Henan, China. She received the B.S. degree in control technology and instrument from Pingdingshan University, China, in 2019. She is currently pursuing the M.S. degree in control engineering with the Xi'an University of Science and Technology. Her research interests include image process and dust detection.

...